



Physicochemical and functional properties of carboxymethylated insoluble dietary fiber of *Lycium barbarum* seed dreg

Jian-Guo Zhang^{a,b}, Gang Yang^a, Wang-Wei Zhang^a, Kiran Thakur^{a,b}, Fei Hu^{a,b},
 Mohammad Rizwan Khan^c, Zhi-Jing Ni^{b,*}, Zhao-Jun Wei^{a,b,*}

^a School of Food and Biological Engineering, Hefei University of Technology, Hefei 230009, People's Republic of China

^b School of Biological Science and Engineering, Ningxia Key Laboratory for the Development and Application of Microbial Resources in Extreme Environments, North Minzu University, Yinchuan 750021, People's Republic of China

^c Department of Chemistry, College of Science, King Saud University, Riyadh 11451, Saudi Arabia

ARTICLE INFO

Keywords:

Lycium barbarum seed dreg
 Insoluble dietary fiber
 Carboxymethylation
 Degree of substitution
 Physicochemical
 Functional properties

ABSTRACT

Lycium barbarum seed dregs (LBSDs) were used for carboxymethyl modification, resulting in three degree of substitution samples (DS). Based on the substitution degree, samples were designated as low degree of substitution insoluble dietary fiber (L-IDF), medium degree of substitution insoluble dietary fiber (M-IDF) and high degree of substitution insoluble dietary fiber (H-IDF). Physicochemical and functional properties of IDFs were examined in relation to carboxymethylation degree. Infrared Fourier transform spectroscopy (FT-IR) confirmed the carboxymethyl group. According to the results, IDF, L-IDF, M-IDF, and H-IDF acquired higher enthalpy changes, and their thermal stability improved significantly. A higher DS resulted in an increase in hydration properties such as water retention capacity and water swelling capacity, as well as functional properties such as glucose adsorption capacity, nitrite ion adsorption capacity, and cholesterol adsorption capacity. As a result, carboxymethylation could effectively enhance the biological properties of *L. barbarum* seed dreg insoluble dietary fiber (LBSDIDF).

1. Introduction

A deciduous shrub, *Lycium barbarum* thrives in northern China, the Mediterranean area, and many temperate zones around the world. Known as the Goji berry or wolfberry, the fruit of *L. barbarum* is widely used as a nourishing tonic in Traditional Chinese Medicine (Zhang et al., 2023). Various parts of this plant have been extensively analyzed for chemical components, and over 200 types of nutrients have been discovered. Some of these components are flavonoids, phenolic acid, polyphenols, and various polysaccharides, which are known for their biological properties (Ma et al., 2023).

Insoluble dietary fiber (IDF) is the most common type of dietary fiber (DF) in grains, fruits, and plant by-products. IDF is largely composed of cellulose, hemicelluloses, and lignin, which contain a variety of functional groups, including alcohols, aldehydes, ketones, carboxylic acids, phenolic bonds, and esters (Meng et al., 2019). Traditional DF treatments, such as alkaline extraction and enzymatic hydrolysis, cannot denature polysaccharide bonds, so they cannot adequately isolate these

moieties.

The industrial application of DFs is largely based on their physicochemical and functional properties, and latter can be modified by extraction approaches and processing conditions (Zheng & Li, 2018). Numerous approaches, including physical, chemical, biological, and hybrid methods have been utilized in the food industry to improve the physicochemical and functional characteristics of DFs. Among them, thermal treatment, high-frequency vibrations, microwave radiation, reduction to small particles, extreme pressure application, and enzymatic cleavage can break down the polysaccharide chains and uncover more functional groups, resulting into structural, chemical, and functional changes in modified DFs (Gan et al., 2020).

Ultrasonic treatment disrupted the microstructure of IDF in garlic straw and introduced hydrophilic groups, thereby created a honeycomb network structure. This transformation could improve both the functional and physicochemical properties of IDF in garlic straw (Huang, Ding, Zhao, Li, & Ma, 2018). In another study, the application of acid hydrolysis process (AHP) was shown to enhance the bile acid binding

* Corresponding author at: School of Food and Biological Engineering, Hefei University of Technology, Hefei 230009, People's Republic of China.

E-mail addresses: zhangjianguo@hfut.edu.cn (J.-G. Zhang), 2021171493@mail.hfut.edu.cn (G. Yang), kumarikiran@hfut.edu.cn (K. Thakur), hufei@hfut.edu.cn (F. Hu), mrkhan@KSU.EDU.SA (M.R. Khan), lovebear@vip.163.com (Z.-J. Ni), zjwei@hfut.edu.cn (Z.-J. Wei).

<https://doi.org/10.1016/j.fochx.2024.101270>

Received 21 November 2023; Received in revised form 4 January 2024; Accepted 5 March 2024

Available online 7 March 2024

2590-1575/© 2024 The Authors. Published by Elsevier Ltd. This is an open access article under the CC BY-NC-ND license (<http://creativecommons.org/licenses/by-nc-nd/4.0/>).

capacity of soluble dietary fiber (SDF) derived from tomato peel (Niu, Li, Xia, Hou, & Xu, 2018). These findings highlight the potential of various modification techniques to optimize the nutritional and health benefits of different types of DFs in food products. Zheng, Tian, Li, Wang, and Shi (2021) used cellulase and hemicellulase to hydrolyze coconut cake DF, which significantly increased the SDF content, water retention capacity (WRC), emulsion stability, glucose dialysis retardation index (GDRI), and bile adsorption capacity (BAC).

In the past years, carboxymethylation modification was found successful for various DFs from wheat bran (Zhang et al., 2019), coconut cake (Zheng et al., 2021), and palm kernel expeller (Zheng, Li, & Tian, 2020) which not only resulted in alteration in chemical composition but also improved the antioxidant activity and functional properties.

This is the first ever study on the carboxymethylation modification of *L. barbarum* seed dreg insoluble dietary fiber (LBSDIDF). Modified IDF with high, medium and low carboxymethylation substitution were obtained based on different degrees of modification. The functional, physicochemical, and structural properties of modified IDF fractions were assessed, revealing a novel method to enhance the nutritive characteristics of modified IDF fractions. Our data set a framework to better understand the properties of modified IDF and also signify the practical application of modified IDF (nutritional ingredients) in food products.

2. Materials and methods

2.1. Materials

L. barbarum seed dreg (LBSD), which is a by-product obtained during the oil extraction process, was sourced from Ningxia Lycium Industry Co., Ltd. (Yinchuan, China). Although it has a low oil content, LBSD is not defatted and instead passed through a sieve with a mesh size of 60 to retain its unique nutritional properties. In addition to the primary reagents used in the present research, all other auxiliary compounds were sourced from the highest quality analytical-grade materials.

2.2. *Lycium barbarum* insoluble dietary fiber preparation

According to previously described method with few modifications, IDF was extracted from LBSD (Guo et al., 2021). The certain mass of LBSD and distilled water were mixed thoroughly in accordance with the 1:10 material-liquid ratio. After that, a certain amount of α -amylase (1.6% of the mass of LBSD) was added at pH 6.0, and the LBSD was hydrolyzed at 60 °C for 40 min in a constant temperature magnetic stirrer. After the temperature was lowered to 40 °C, a certain amount of protease (0.8% by mass of LBSD) was added to the mixed solution and stirred at 40 °C for 120 min. To inactivate the enzyme, we incubated it at 100 °C for up to 5 min which was followed by cooling and centrifugation of the samples at 8000 rpm for 20 min. The precipitate was collected, washed multiple times with 4% sodium hydroxide and hot water at 70 °C followed 95% ethanol. The precipitated sample, which is called IDF, was obtained by drying the substance at 55 °C in an incubator until it reached a stable weight.

2.3. Modification of *Lycium barbarum* dietary fiber

As per previous methodology with modifications (Zhang et al., 2019), three portions of 1.0 g of LBSDIDF were weighed into 30 mL of ethanol solution followed by the addition of a certain amount of 6/5/4.5 mol/L NaOH solution and stirring the reaction for 1 h at 40 °C under a constant temperature magnetic stirrer. Then, 3/4/3 g of chloroacetic acid was added at 60 °C and the solution was stirred for 3/3/4.5 h. Following the completion of the reaction, the solution was subjected to a cooling process until it reached a temperature of 25 °C, and then the mixture was adjusted to neutral with glacial acetic acid, the sediment was then washed three times by filtration with 95% ethanol and acetone.

After washing, the precipitate was placed in a Petri dish, and then the Petri dish was dried in a blast oven to a constant weight to obtain three kinds of samples with low, medium, and high degree of substitution (DS), and the obtained samples were named as L-IDF, M-IDF, and H-IDF.

2.4. Degree of substitution analysis

According to the previous methodology of (Li et al., 2017) with minor modifications, accurately weighed 0.5 g of the sample was placed in a 50 mL beaker and 40 mL of 2 mol/L HCl solution was added. And after stirring on a constant temperature magnetic stirrer for 180 min without obvious lumps, the sample was filtered with a quartz sand glass funnel, until the filtered filtrate was free of chloride ions. Then the product was dissolved in 0.1 mol/L NaOH standard solution under slightly hot condition; when the solution was transparent, phenolphthalein was used as indicator and titrated with 0.1 mol/L standard HCl solution immediately. The DS of IDF was calculated using Eqs. (1) and (2).

$$A = (C_1V_1 - C_2V_2)/m \quad (1)$$

$$DS = 0.162A/(1 - 0.058A) \quad (2)$$

Where: the quantity of acidic substance ingested per unit weight of the specimen is referred to as A, mol/g; C_1 is the concentration of NaOH standard solution for dissolved dietary fiber, 0.1 mol/L; V_1 is the volume of NaOH standard solution for dissolved dietary fiber, mL; C_2 is the concentration of HCl standard solution, 0.1 mol/L; V_2 is the volume consumed for titrating HCl standard solution, mL; m is the dietary fiber sample mass, g; 162 is the molar mass of the dehydrated glucose unit of cellulose, g/mol; 58 is the net increase in molar mass of the dehydrated glucose unit for each substituted carboxymethyl, g/mol.

2.5. Structural characterization

2.5.1. Fourier transform infrared spectroscopy (FT-IR)

To obtain the molecular structure of IDFs, FT-IR spectroscopy was performed as described in the previously reported method. For spectral analysis, we scanning over a wide range of frequencies between 400 and 4,000 cm^{-1} to obtain precise measurements of each sample (Zhang, Xu, Cao, & Liu, 2023).

2.5.2. Differential scanning calorimetry (DSC)

The thermal properties of the IDFs were evaluated according to the method given by (Wang et al., 2017) using 3.0 mg of sample from room temperature to 400 °C at a speed of 15 °C/min. To determine the change in heat flow during the experiment, we used a state-of-the-art differential scanning calorimeter (model Q2000, manufactured by TA Instruments, based in Wilmington, America). Specifically, the heat flow between the samples was monitored, and clean and empty aluminum pan was used to ensure accurate and precise measurements throughout our testing process.

2.5.3. Scanning electron microscopy (SEM) evaluations

SEM (JSM-6490LV) was used for micrographic analysis of IDFs. Powder cases were placed on a metal stage using the electrically conducted tape method and sputtering of gold was performed before images of each sample were taken at three magnifications of 200, 500, and 1000 \times . (Zhang et al., 2019).

2.6. Physicochemical properties

2.6.1. Water retention capacity (WRC)

The WRC of the samples was determined according to the previously described method with slight modifications (Wang et al., 2017). During sample processing, 1.0 g of dried sample and 20 mL of distilled water were mixed, and the mixture was left undisturbed at a constant

temperature for 24 h. Subsequently, the samples were mixed and centrifuged at 6000 rpm for approximately 15 min. Further, the residues were collected, and after accurate weighing, the WRC values were calculated using Eq. (3):

$$\text{WRC}(\text{g/g}) = (W_2 - W_1)/W_1 \quad (3)$$

In Eq. (3), W_2 signifies the weight of the residue obtained after accounting for water content, while W_1 corresponds to the mass of the sample after drying.

2.6.2. Water swelling capacity (WSC)

For this, 2.0 g of the sample was placed in a 100 mL tube and 50 mL of deionized water was added and mixed for 24 h according to previously described method with few modifications (Wang et al., 2017). WSC was calculated using Eq. (4):

$$\text{WSC}(\text{ml/g}) = (V_2 - V_1)/W_0 \quad (4)$$

In Eq. (4), V_2 designates the volume (in mL) of dietary fiber once water has been added to it, while V_1 signifies the volume (in mL) of dietary fiber without any added water. Additionally, W_0 represents the mass of dietary fiber without any added water, measured in grams.

2.6.3. Oil retention capacity (ORC)

1.0 g of the desiccated sample with 25 mL of soybean oil was mixed in a centrifuge tube and allowed to stir for a duration of 1 h. Following an initial centrifugation process at 3,000 rpm for 20 min, the top layer of oil was removed, the residue was drained on filter paper, and then accurately weighed. Using Eq. (5), the ORC was determined (Zheng & Li, 2018):

$$\text{ORC}(\text{g/g}) = (W_2 - W_1)/W_1 \quad (5)$$

In Eq. (5), W_2 represents the weight (in grams) of the residue containing oil, while W_1 refers to the weight (in grams) of the dry sample.

2.7. Functional properties

2.7.1. Cation exchange capacity (CEC)

We determined the cation exchange capacity using a modified method of (Zhang et al., 2019). To begin, dried samples (1.0 g) were added to HCl (0.1 mol/L, 60 mL) and allowed to stand for 24 h. After collection and thorough washing, residues were dried at 55 °C until a consistent weight was obtained. 0.1 g amount of the extracted powder was mixed with NaCl (5%, 100 mL). Subsequently, the compound was titrated with a 0.01 mol/L solution of NaOH followed by the addition of phenolphthalein (2.0 g/L) as the color indicator. The volume of NaOH solution consumed was determined through a blank test where distilled water was used in place of hydrochloric acid. Finally, the CEC of the resulting samples was determined according to Eq. (6):

$$\text{CEC}(\text{mmol/g}) = 0.01 \cdot (V_2 - V_1)/W_1 \quad (6)$$

The calculation for titrated sample volume (V_2), titrated blank volume (V_1), sodium hydroxide concentration (0.01 mol/L), and sample dry weight (W_1) is as follows.

2.7.2. Cholesterol adsorption capacity (CAC)

According to (Yang, Wu, Cao, Wang, & Zhang, 2019), mixed egg yolk and deionized water were mixed in the ratio of 1:9 (v/v) and the mixture was carefully stirred into a homogeneous emulsion. After preparing the finished yellow emulsion, the dried sample was added to the mixture at a ratio of 1:5 (w/v). To accurately simulate the conditions of the human stomach, the pH of our mixture was carefully adjusted to a level of 2.0, or the small intestine (pH 7.0). The obtained solution was incubated at 37 °C for 120 min, followed by centrifugation at 4000 g and 25 °C for 15 min. After obtaining the supernatant, the o-phthalaldehyde method was utilized for the determination of cholesterol concentration. To

determine the CAC of sample, we used Eq. (7).

$$\text{CAC}(\text{mg/g}) = (C_1 - C_2)/M \quad (7)$$

The cholesterol content in the egg yolk (mg) is represented by C_1 , the cholesterol content in the supernatant (mg) is represented by C_2 , and the weight of the test sample (g) is represented by M .

2.7.3. Glucose adsorption capacity (GAC)

To determine GAC, a previously described protocol was used (Song, Su, & Mu, 2018). For this, samples weighing 0.1 g was dispersed into glucose solution (500 mg/L, 20 mL) and stirred for 6 h at 37 °C. After centrifuging at 4000 r/min for 15 min, DNS colorimetric method was used to measure glucose concentration in the supernatant. The GAC was calculated using the following formula (8):

$$\text{GAC}(\text{mg/g}) = (W_2 - W_1)/W_0 \quad (8)$$

Eq. (8) is used to calculate the total glucose content in the solution (in milligrams), based on the weight of the sample (W_0) and the level of glucose in the solution (W_2) and supernatant (W_1).

2.7.4. Nitrite ion adsorption capacity (NIAC)

According to (Zhu et al., 2018) with slight modifications, NIAC of dried samples (weighing 1.0 g) was determined. To simulate the conditions of the stomach and small intestine, a solution of NaNO_2 (25 mL, 100 $\mu\text{M/L}$) was added, and the pH level was adjusted to 2.0 and 7.0, respectively. After combining the mixture, it was subjected to agitation at 37 °C for 2 h. Then after, mixture was centrifuged at 4000 rpm for a duration of 15 min. After obtaining the supernatant, the concentration of nitrite ions was measured by the naphthylamine hydrochloride assay and the NIAC was calculated using a specific Eq. (9).

$$\text{NIAC}(\mu\text{mol/g}) = (n_2 - n_1)/w_0 \quad (9)$$

In Eq. (9), n_2 denotes the concentration (in grams) of nitrite ion content in solution, while n_1 represents the concentration (in grams) after adsorption has taken place. Additionally, w_0 refers to the weight (in grams) of the sample used in the experiment.

2.8. Antioxidant properties

2.8.1. Extraction of antioxidant substances

Following the procedure outlined in the study by Zhang et al. (2019), 1.0 g of DF sample was placed in a conical flask followed by the addition of 10 mL of 80% ethanol solution for extraction using ultrasonic treatment for a certain time.

2.8.2. Total phenolic content (TPC)

For the quantification of total phenolic content in the samples, the colorimetric method of forintanol was employed. For this, 0.5 mL of the extract was added to 0.5 mL of Forinol reagent along with 7.5 mL of distilled water. The obtained solution was gently mixed and allow to complacently stand at room temperature for 10 min. Then, the resulting mixture was supplemented with 3 mL of a solution composed of 20% Na_2CO_3 (w/v) and stirred until completely homogenized. The obtained sample was transferred to a constant temperature bath, maintained at a steady degree of 40 °C for 20 min, followed by an immediate absorbance measurement (A_{765}). The standard curve was plotted against a standard solution of gallic acid by the colourimetric method of forintanol. The relative total phenolic content was determined by comparison with a standard solution of gallic acid (Singleton, Orthofer, & Lamuela, 1999).

2.8.3. Total reducing power

At first, 0.4 mL of extract solution was combined with 2.5 mL of phosphate buffer (pH level of 6.6) as well as 2.5 mL of 1% potassium ferricyanide. Then, the mixture was placed into a temperature-controlled water bath operating at 50 °C for 20 min. Subsequently,

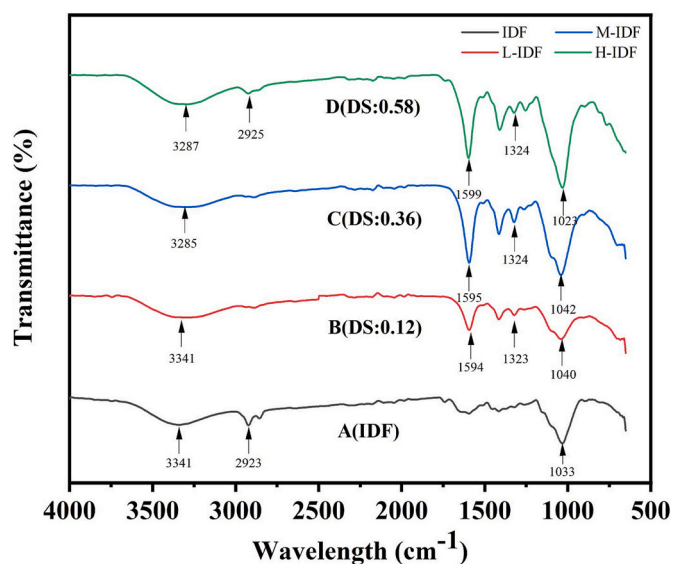


Fig. 1. FT-IR spectra of IDF and its carboxymethylated derivatives with different DS values. (A) the native sample of IDF, (B–D) the carboxymethylated derivatives with different DS values.

2.5 mL of 10% TCA reagent was added. After thorough mixing, the sample was centrifuged at 6000 r/min for 10 min. Once completed, 2.5 mL of the supernatant was taken out and added to another tube containing 2.5 mL of distilled water and 0.5 mL of 0.1% ferric chloride. The resulting mixture was allowed to react for 10 min before the final measurement (Zhang et al., 2019).

2.8.4. ABTS⁺ radical scavenging activity

For this, 4 mL of ABTS working solution was added to 1 mL of extraction solution in a test tube and allowed to react for 5 min without the direct light exposure. A_1 was obtained by determining its absorbance value at 734 nm. Instead of ABTS working solution, 4 mL of pH 4.5 buffer was used to measure the absorbance values as control A_2 , and to obtain the absorbance values for blank group A_0 (anhydrous ethanol was utilized instead of the extraction solution). In order to establish the relative ABTS⁺ radical scavenging ability of the samples, VC standard solutions were used as a comparison (Zhou et al., 2018).

2.8.5. DPPH radical scavenging activity

To begin, 1 mL of extract solution was placed into a test tube followed by supplementing the mixture with 4 mL of 0.1 mmol/L DPPH working solution which was allowed to react for 30 min without the direct light exposure. The measurement of absorbance was conducted at 517 nm for the A_1 sample group. The absorbance value of control A_2 was measured with 4 mL of anhydrous ethanol instead of DPPH working solution; anhydrous ethanol was used instead of the extract, and the blank group A_0 was calculated to establish the absorbance value. The VC

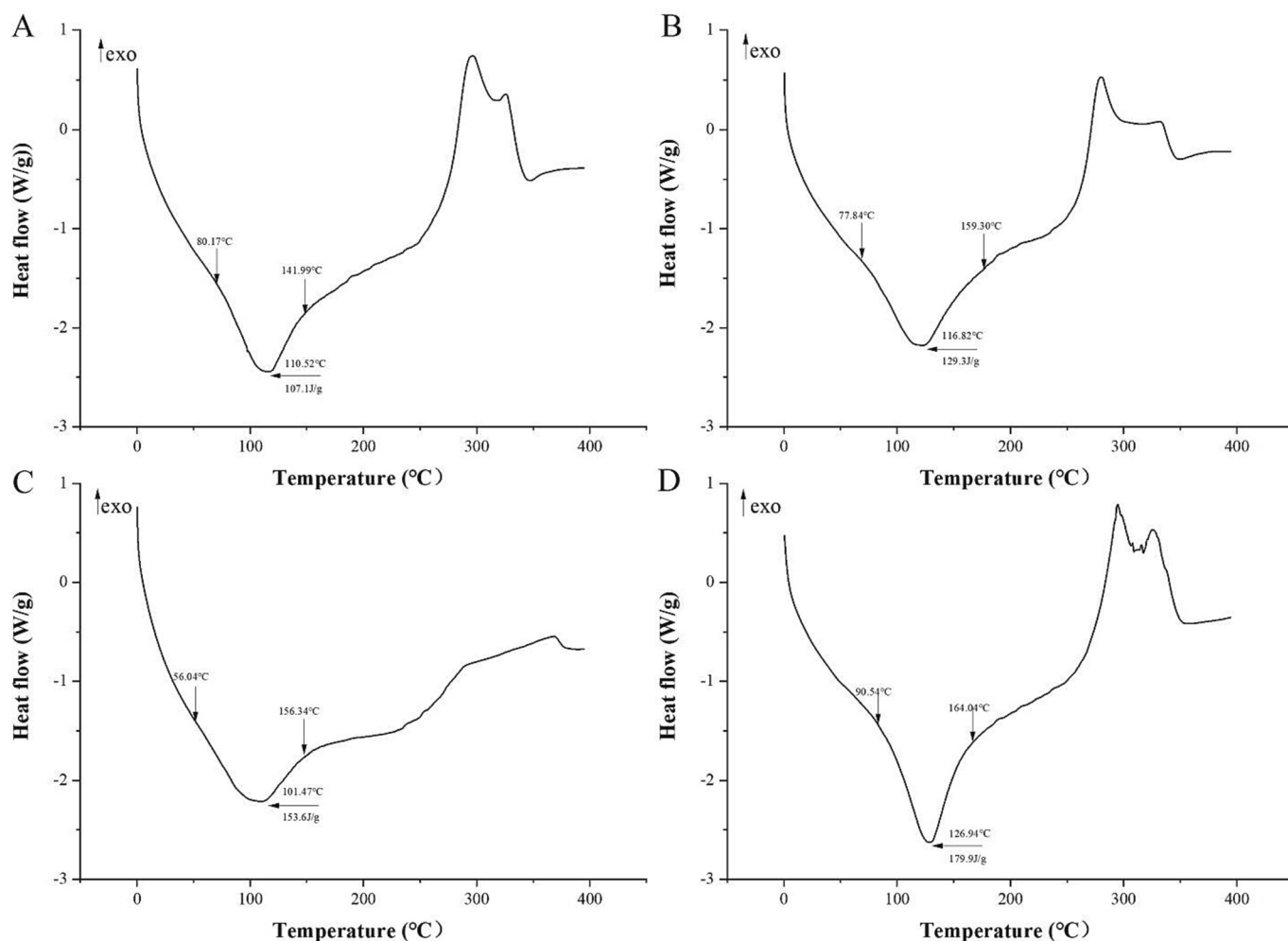


Fig. 2. DSC properties of DFs. (A) IDF, (B) L-IDF, (C) M-IDF, (D) H-IDF.

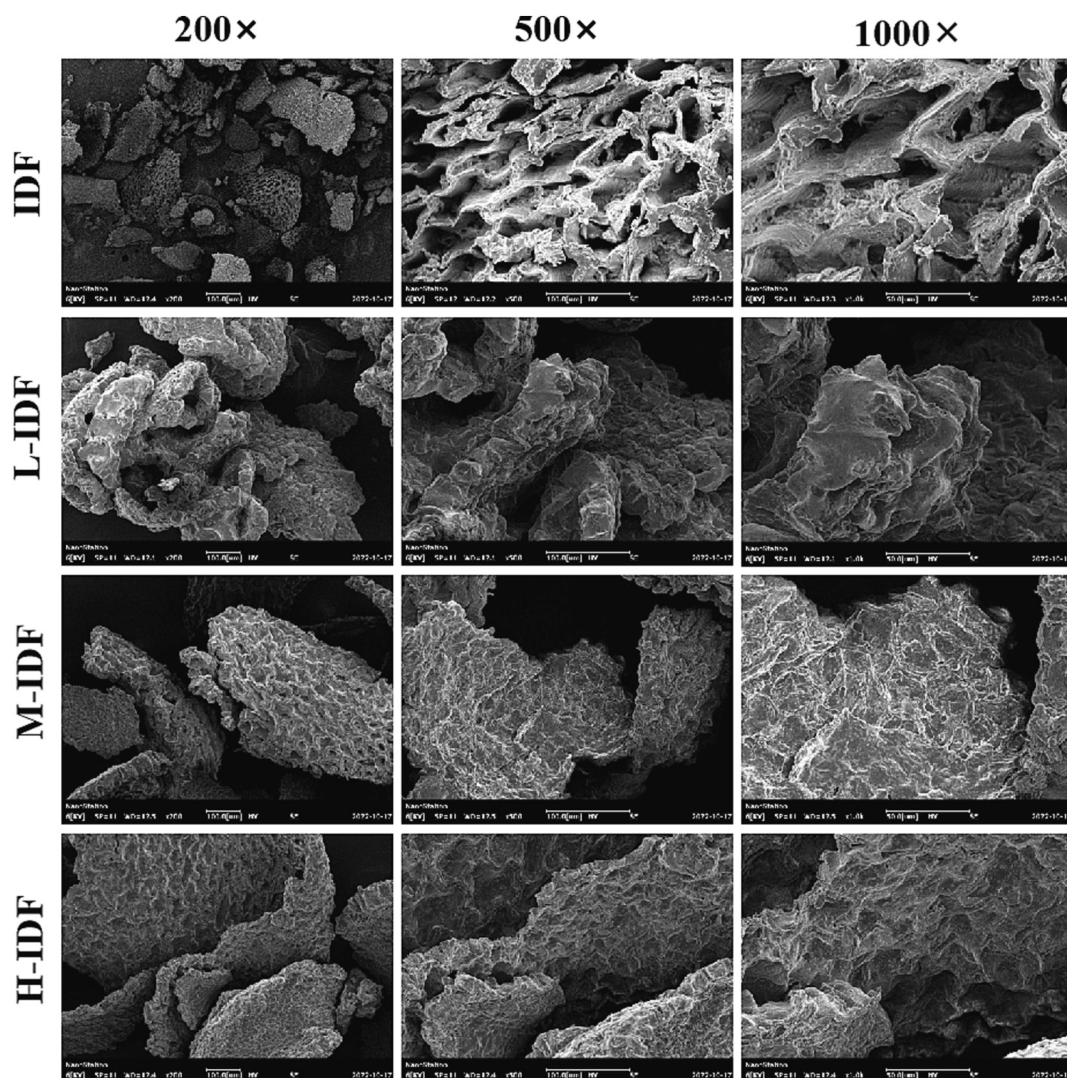


Fig. 3. Scanning electron micrographs of dietary fibers. IDF (200 \times , 500 \times and 1000 \times), L-IDF (200 \times , 500 \times and 1000 \times), M-IDF (200 \times , 500 \times and 1000 \times) and H-IDF (200 \times , 500 \times and 1000 \times) at magnification.

standard solution was compared to determine the relative •DPPH radical scavenging ability of the samples (Chrysargyris, Panayiotou, & Tzortzakis, 2016).

2.8.6. Fe^{2+} chelating activity

For this, 2.0 mL of extraction solution was added to 0.1 mL of 2 mmol/L $FeSO_4$ solution and 0.2 mL of 5 mmol/L phenazine solution and stirred well for 10 min at room temperature, and the absorbance was determined at 562 nm. The relative ferrous ion chelating capacity of the samples was determined by comparison with EDTA-2Na standard solution (Li et al., 2018).

3. Results and discussion

3.1. Structural characterization

3.1.1. Fourier transform infrared analysis

The IR spectra of IDF and different carboxymethyl modified IDFs are shown in Fig. 1. All the IDFs showed a broad vibration absorption peak in the range of 3500 cm^{-1} –3000 cm^{-1} , which is mainly generated by the stretching of hydrogen and hydroxyl groups bound to O–H produced by cellulose and hemicellulose (Zhao et al., 2013). The absorption peak near 2925 cm^{-1} is a C–H stretched vibration and the absorption peak

near 1033 cm^{-1} is caused by a symmetric stretching vibration of (–C–O–C–). Compared with the unmodified IDFs, the modified IDFs exhibited new and stronger absorption peaks, which were mainly distributed around 1595 cm^{-1} and 1324 cm^{-1} . The asymmetric C=O stretching vibration in carboxymethyl is responsible for the absorption peak near 1595 cm^{-1} , and the in-plane variable angle vibration of O–H is responsible for the absorption peak around 1324 cm^{-1} . The results showed that COO– groups were successfully introduced into the modified IDFs molecules. The introduction of these new bonds indicates the etherification reactions in IDFs and ensures the carboxymethyl modification, resulting into stronger absorption peak of C=O as the degree of substitution increased.

3.1.2. Thermal properties

DSC is programmed to control the temperature change and measure the power difference (heat flow rate) of the samples or reference versus temperature. The thermal properties of DFs were demonstrated by DSC, as shown in Fig. 2. According to the shape of the curves, all the samples were exothermic during melting. The results showed that IDF, L-IDF, M-IDF, and H-IDF have a characteristic peak in the 0–400 $^{\circ}C$ interval. Different IDFs displayed varying peak temperatures, with values observed at 110.52 $^{\circ}C$, 116.82 $^{\circ}C$, 101.47 $^{\circ}C$, and 126.94 $^{\circ}C$, respectively. Compared with the enthalpy change value of 107.1 J/g for IDF,

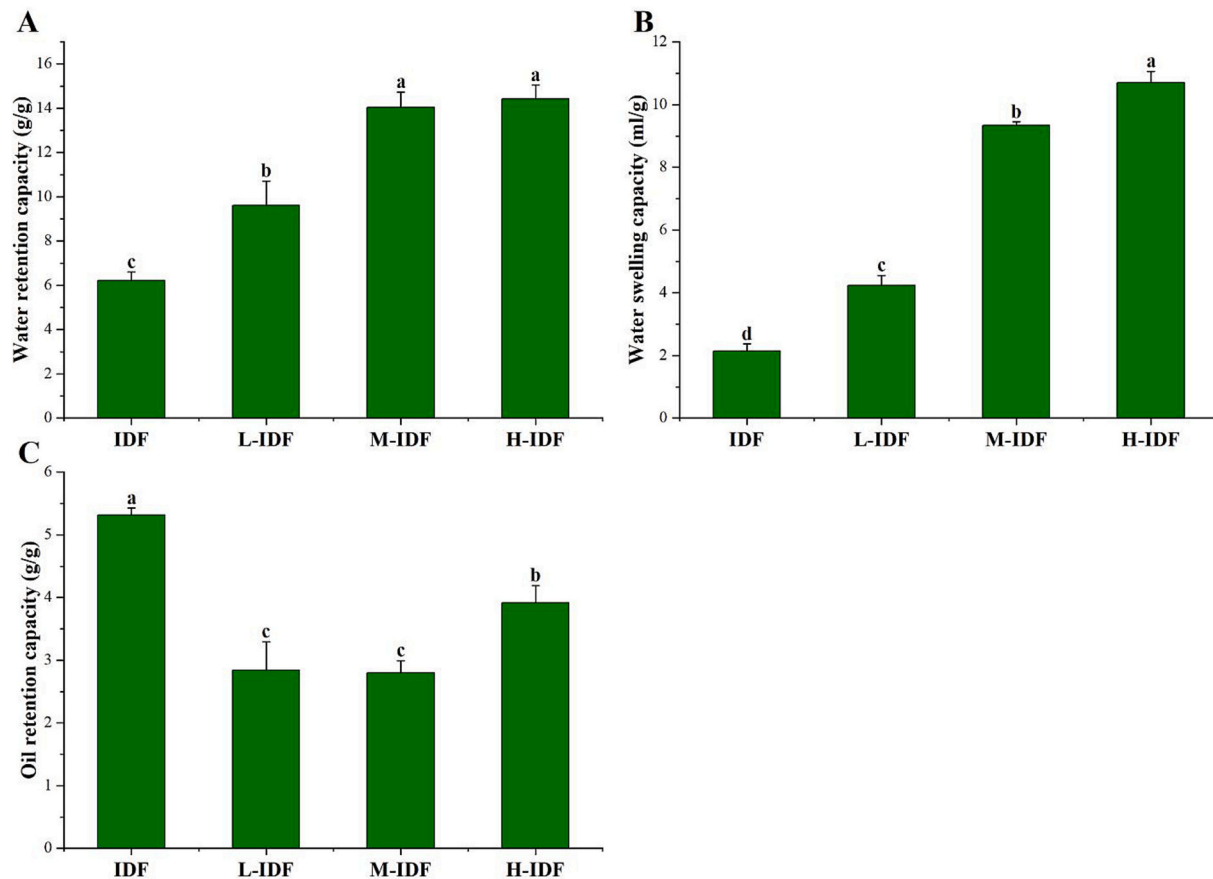


Fig. 4. Physicochemical properties of modified and unmodified DFs. Water holding capacity (A), water absorption and swelling capacity (B), oil holding capacity (C). Data were expressed as means \pm standard deviations ($n = 3$) with different letters representing significant difference ($P < 0.05$).

the enthalpy changes values of L-IDF, M-IDF, and H-IDF were significantly higher, 129.3 J/g, 153.6 J/g and 179.9 J/g, respectively. The enthalpy change (ΔH) may be related to the hydrogen bonding in the substance (Ji et al., 2019). The results suggest that the solid-liquid phase change requires more heat, and that the carboxymethylation modification enhances the thermal stability of IDFs. Increasing the DS of IDFs results in a corresponding improvement in its thermal stability (An et al., 2014). These findings highlight the potential of modified IDFs to enhance the thermal stability of foods within the food industry. By optimizing the DS of IDFs, food manufacturers may be able to improve the shelf life and overall quality of food products.

3.1.3. Surface microstructure characters

The surface microstructure of IDFs is shown in Fig. 3, revealing a relatively fine fragment structure with a sparse and porous surface and a complex spatial network structure. After carboxymethylation modification, the sample changed to a honeycomb appearance, showing a loose and multi-chip microstructure with more cracks, probably due to the destruction of cellulose during the carboxymethylation process (Zheng et al., 2020). In simpler terms, it has been found through studies that the way in which IDFs are internally structured and their surface properties, play a significant role in their absorption activity. Another noteworthy point is that certain physicochemical properties, such as water retention and oil absorption, are associated with the loose network structure of IDFs (Dong, Wang, Lü, Zhu, & Shen, 2019). Such findings can help us understand the key role of IDF in promoting digestive health. As the degree of modification increased, the looser the surface morphology of the dietary fibers appeared, positively influencing the activity and properties of the samples. This may explain the improved hydration properties, adsorption properties, and physiological

activity of the modified IDFs.

3.2. Hydration properties

3.2.1. Water retention capacity and water swelling capacity (WRC and WSC)

The hydration characteristics of IDFs before and after modification are depicted in Fig. 4. As shown in Fig. 4A and B, the WRC and WSC of the modified IDFs were significantly higher compared to IDF, consistent with the results that carboxymethylated bran dietary fiber elevated WRC and WSC (Li et al., 2021), and had a tendency to increase with the increase of DS. Several factors influence the WRC and WSC of IDFs, including the number of hydrophilic groups, the conformation of the glycan chains, the size of the particles, and the surface structure (Pérez-Jiménez, Díaz-Rubio, Mesías, Morales, & Saura-Calixto, 2014). Due to the carboxymethylation reaction of IDFs, IDF molecules undergo increased hydrophobicity due to the inclusion of carboxymethyl groups into their structure. The carboxymethylation process leads to etherification of the hydroxyl groups in the IDFs, resulting in increased hydrophilicity due to the presence of carboxymethyl groups. In addition, the porous honeycomb structure of IDFs (shown in Fig. 3) also contributed to WSC and WHC (Qi et al., 2016).

3.2.2. Oil retention capacity (ORC)

The ORCs of L-IDF (2.84 g/g), M-IDF (2.79 g/g), and H-IDF (3.92 g/g) were remarkably lower ($P < 0.05$) compared to the unmodified IDF, as shown in Fig. 4C, which is consistent with the findings of (Zheng et al., 2021). Although more porous structures were responsible for increased ORCs of DFs (Zhang et al., 2019), carboxymethylated IDFs possessing honeycomb microstructures all exhibited lower ORCs than

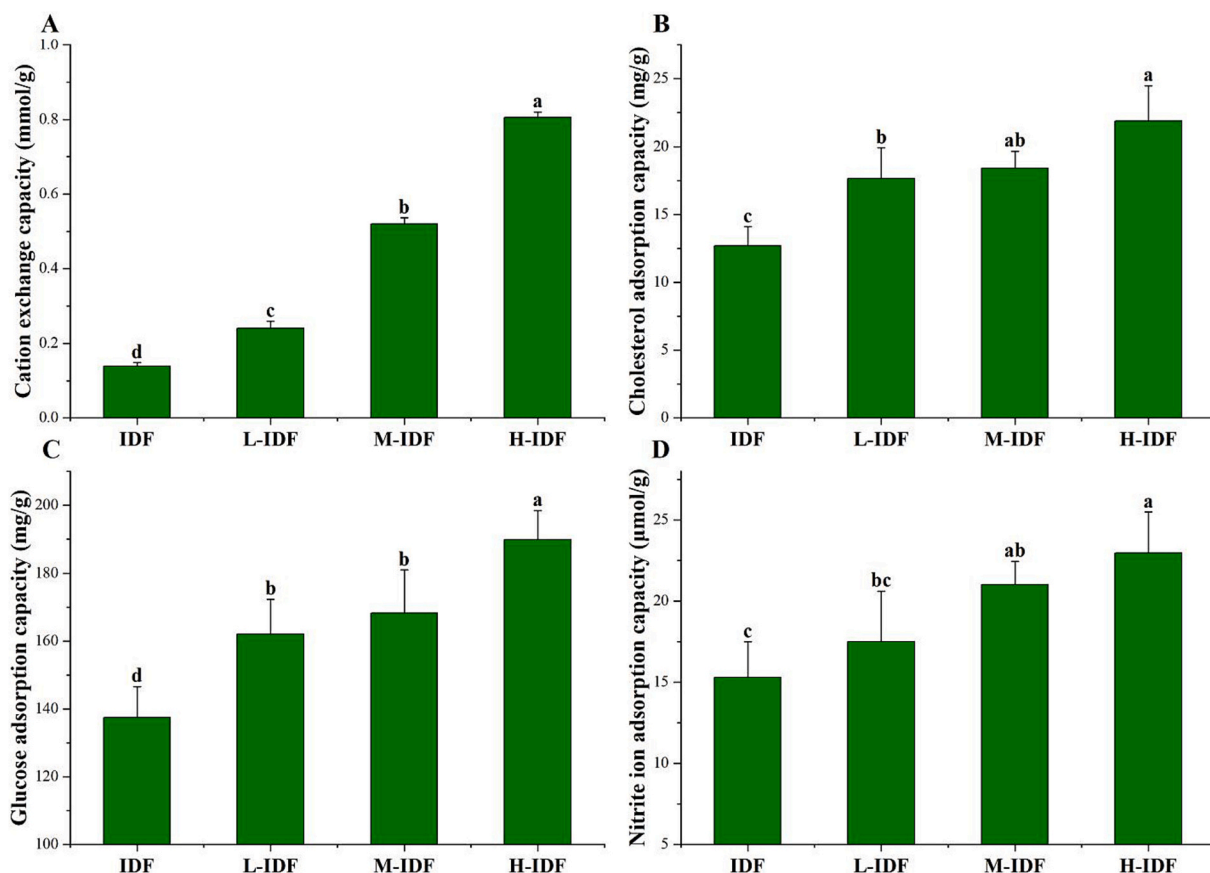


Fig. 5. Functional properties of modified and unmodified DF. Cation exchange capacity (A), glucose adsorption capacity (B), nitrite ion adsorption capacity (pH 2.0) (C) and cholesterol adsorption capacity (pH 2.0) (D). Data were expressed as means \pm standard deviations ($n = 3$) with different letters representing significant difference ($P < 0.05$).

IDFs ($P < 0.05$), possibly due to hydrophobicity or a reduction in specific surface area.

3.3. Functional properties

3.3.1. Cation exchange capacity (CEC)

The data in Fig. 5A showed that IDF has certain cation exchange ability, and the carboxymethylation modification can effectively improve the CEC of IDF ($P < 0.05$). It has been shown that the structure of IDFs contains some carboxyl and hydroxyl side chain groups of glyoxalate, which can undergo exchange reactions with organic cations (Kumar & Malviya, 2023). It was readily observed that the cation exchange capacity of IDF escalated in proportion to the increase in DS. This analysis identifies the increase in hydroxyphenol and carboxyl group numbers within the polysaccharide molecule as a possible reason for this effect, possibly resulting from carboxymethylation (Y. Wang et al., 2020), with higher DS and higher number, which leads to a stepwise increase in cation exchange capacity.

3.3.2. Cholesterol adsorption capacity (CAC)

In a recent study, it was found that consuming more DF can lower serum cholesterol levels, and is linked with a decreased risk of cardiovascular diseases. Fig. 5B depicted the CAC of IDF, L-IDF, M-IDF, and H-IDF at pH 2.0 ($P < 0.05$), while no adsorption capacity was observed at pH 7.0. According to these findings, it appears that the intestine is more effective in absorbing cholesterol than the stomach (Huang, Ma, Tsai, & Chang, 2019), suggesting that the adsorption capacity of DF on cholesterol was greatly influenced by the pH of the system, indicating a greater effect of pH. The possible reason for this can be that the introduced carboxymethyl group enhances the spatial site resistance of the

fiber molecules, thus increasing the interaction between the fiber and the hydrophobic agent (Zheng et al., 2022). Along with the introduction of a significant number of carboxyl groups by carboxymethylation modification, carboxymethylation proved to be more effective in the adsorption of carboxyl groups as the main adsorption sites.

3.3.3. Glucose adsorption capacity (GAC)

DFs have the inherent glucose absorption ability, serving as a supportive measure in reducing blood glucose levels in human body (Chau, Wang, & Wen, 2007; Yu, Bei, Zhao, Li, & Cheng, 2018) found that viscosity, porosity, and specific surface area were closely related to the glucose adsorption capacity of DFs. As shown in Fig. 5B, all four samples showed strong glucose adsorption capacity, and the GAC of L-IDF (162.10 mg/g), M-IDF (168.25 mg/g) and H-IDF (189.93 mg/g) were all elevated to some extent ($P < 0.05$) compared to IDF (150.20 mg/g). The main reason can be the introduction of the carboxymethyl group, which is more polar and has a relatively strong affinity for the glucose molecule, the higher the DS, the more carboxymethyl groups leading to a stronger adsorption capacity for glucose (Zheng et al., 2022).

3.3.4. Nitrite ion adsorption capacity (NIAC)

In the intestine, NO_2^- has the potential to react with tertiary or secondary amines and amides, resulting in the creation of N-nitrosamines (Xu et al., 2022), and nitrosamines have been recognized as carcinogens. In human beings, the NIAC present in DF typically acts as a safeguard against the toxicity that might arise from excessive nitrite consumption (Song et al., 2018). NIAC of IDFs was measured *in vitro* in simulated gastric (pH 2.0) and small intestinal (pH 7.0) environments. According to the experimental results, the samples demonstrated minimal adsorption capacity when subjected to a simulated pH 7.0

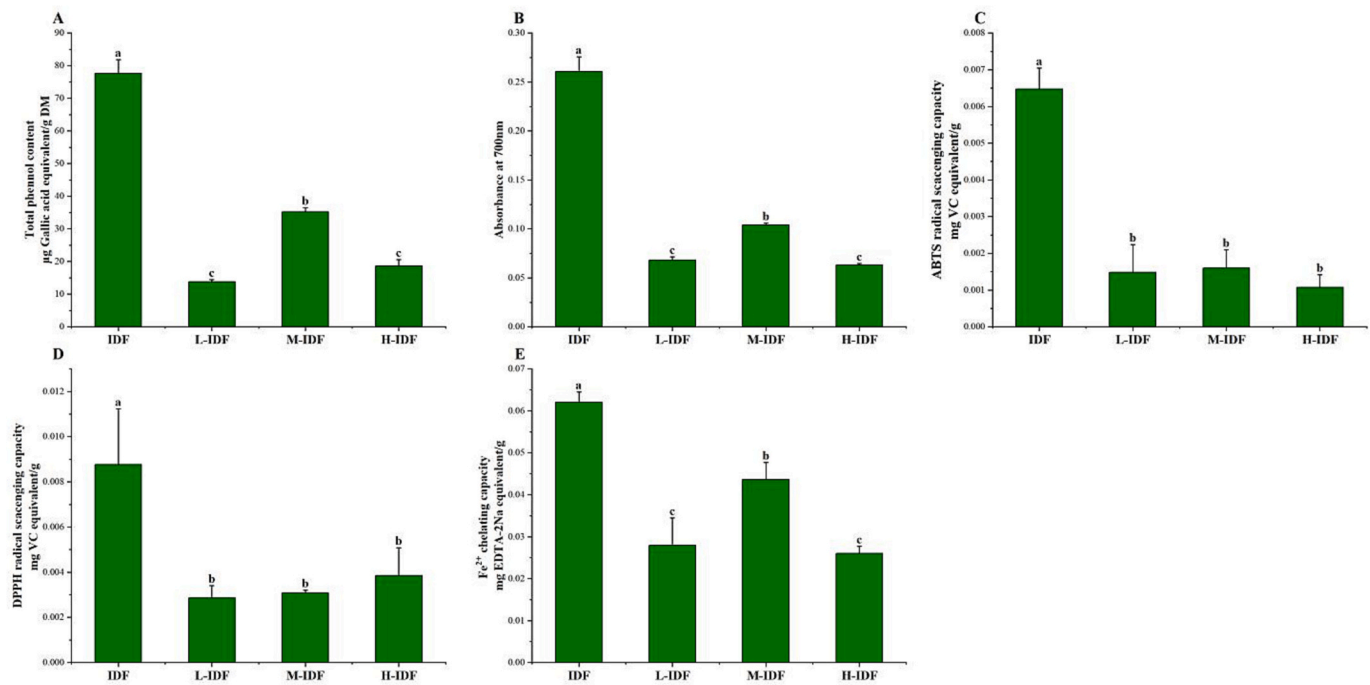


Fig. 6. Antioxidant properties of modified and unmodified IDF. Total phenolic content (A), total reducing power (B), ABTS⁺ radical scavenging capacity (C), •DPPH radical scavenging capacity (D) and Fe²⁺ chelating capacity (E). Data were expressed as means \pm standard deviations (n = 3) with different letters representing significant difference ($P < 0.05$).

environment that mimics the small intestine. At higher pH, the density of negative charges on the surface of DFs tends to increase which can lead to the repulsion of nitrite ions, resulting in a weaker NIAC due to a decrease in the interaction between the two.

Fig. 5C showed the results of the assay under simulated gastric (pH 2.0) conditions. The NIAC of DFs was increased markedly after modification ($P < 0.05$). The reason may be that carboxymethylation treatment can disrupt the β -glycosidic bond and expose more carboxyl and hydroxyl phenols. And the number of carboxyl groups was positively correlated with the DS, which could improve the NIAC.

3.4. Antioxidant properties

To investigate the effect of modification on the antioxidant activity of IDF, *in vitro* antioxidant activities, including •DPPH radical scavenging capacity, ABTS⁺ radical scavenging capacity, ferrous ion chelating capacity, and total reducing power were measured. Fig. 6 displayed the results obtained for the total phenolic content both pre- and post-modification. Compared to IDF, the modified IDFs exhibited significantly lowered antioxidant activity and total phenolic content, as per the obtained results. Studies have suggested that the decline in antioxidant capacity could be attributed to polyphenol removal (Xu et al., 2020). It has been demonstrated that sodium hydroxide treatment is effective in releasing bound phenolic compounds (Yin et al., 2022). The extraction of IDF as well as the modification process in this study involved an alkaline environment, thus invariably leading to a decrease in polyphenol content, and latter is the main cause of free radical scavenging activity (Tan, Lan, Chen, Zhong, & Li, 2023). These data clearly show that the reduction in antioxidant activity after modification may be due to the removal of bound polyphenols, which significantly affected the antioxidant properties of IDF.

4. Conclusion

In this study, the IDF was modified by carboxymethyl modification to obtain three degrees of substitution of carboxymethylated IDFs. FTIR

spectra showed the introduction of a new carboxymethyl group, indicating successful modification. The enthalpies of the three substitution degree samples after the modification were 129.3 J/g, 153.6 J/g, and 179.9 J/g, respectively, which significantly improved the thermal stability of IDF. Carboxymethyl modifications could effectively improve the hydration properties of IDF, including WRC, WSC, and ORC. The functional features of IDF, such as CEC, GAC, NIAC, and CAC were also significantly enhanced. LBSDIDF as well as its carboxymethylated derivatives have the potential to be recognized as a food grade functional ingredient in the food industry.

CRediT authorship contribution statement

Jian-Guo Zhang: Resources, Methodology, Investigation. **Gang Yang:** Writing – original draft, Resources, Investigation. **Wang-Wei Zhang:** Methodology, Formal analysis, Data curation. **Kiran Thakur:** Writing – review & editing, Validation, Methodology. **Fei Hu:** Resources, Formal analysis, Data curation. **Mohammad Rizwan Khan:** Funding acquisition, Writing – review & editing. **Zhi-Jing Ni:** Resources, Methodology, Investigation. **Zhao-Jun Wei:** Writing – review & editing, Supervision, Funding acquisition, Conceptualization.

Declaration of competing interest

There is no declaim.

Data availability

No data was used for the research described in the article.

Acknowledgement

This study was supported by the National Natural Science Foundation of Ningxia Province (2022AAC03230), the National Key Research & Development Program of China (2022YFF1100305), and the Major Projects of Science and Technology in Anhui Province

(202203a06020009), and the Researchers Supporting Project number (RSP2024R138) King Saud University, Riyadh, Saudi Arabia.

References

- An, Y., Cui, B., Wang, Y., Jin, W., Geng, X., Yan, X., & Li, B. (2014). Functional properties of ovalbumin glycosylated with carboxymethyl cellulose of different substitution degree. *Food Hydrocolloids*, 40, 1–8. <https://doi.org/10.1016/j.foodhyd.2014.01.028>
- Chau, C. F., Wang, Y. T., & Wen, Y. L. (2007). Different micronization methods significantly improve the functionality of carrot insoluble fibre. *Food Chemistry*, 100(4), 1402–1408. <https://doi.org/10.1016/j.foodchem.2005.11.034>
- Chrysargyris, A., Panayiotou, C., & Tzortzakis, N. (2016). Nitrogen and phosphorus levels affected plant growth, essential oil composition and antioxidant status of lavender plant (*Lavandula angustifolia* mill.). *Industrial Crops and Products*, 83, 577–586. <https://doi.org/10.1016/j.indcrop.2015.12.067>
- Dong, J. L., Wang, L., Lü, J., Zhu, Y. Y., & Shen, R. L. (2019). Structural, antioxidant and adsorption properties of dietary fiber from foxtail millet (*Setaria italica*) bran. *Journal of the Science of Food and Agriculture*, 99(8), 3886–3894. <https://doi.org/10.1002/jsfa.9611>
- Gan, J., Huang, Z., Yu, Q., Peng, G., Chen, Y., Xie, J., ... Xie, M. (2020). Microwave assisted extraction with three modifications on structural and functional properties of soluble dietary fibers from grapefruit peel. *Food Hydrocolloids*, 101, Article 105549. <https://doi.org/10.1016/j.foodhyd.2019.105549>
- Guo, Y., Byambasuren, K., Liu, X., Wang, X., Qiu, S., Gao, Y., & Wang, Z. (2021). Extraction, purification, and characterization of insoluble dietary fiber from oat bran. *Transactions of Tianjin University*, 27(5), 385–393. <https://doi.org/10.1007/s12209-019-00224-9>
- Huang, L., Ding, X. N., Zhao, Y. S., Li, Y. X., & Ma, H. L. (2018). Modification of insoluble dietary fiber from garlic straw with ultrasonic treatment. *Journal of Food Processing and Preservation*, 42(1). <https://doi.org/10.1111/jfpp.13399>
- Huang, Y. L., Ma, Y. S., Tsai, Y. H., & Chang, S. K. (2019). *In vitro* hypoglycemic, cholesterol-lowering and fermentation capacities of fiber-rich orange pomace as affected by extrusion. *International Journal of Biological Macromolecules*, 124, 796–801. <https://doi.org/10.1016/j.ijbiomac.2018.11.249>
- Ji, Y. H., Liao, A. M., Huang, J. H., Thakur, K., Li, X. L., & Wei, Z. J. (2019). Physicochemical and antioxidant potential of polysaccharides sequentially extracted from *Amana edulis*. *International Journal of Biological Macromolecules*, 131, 453–460. <https://doi.org/10.1016/j.ijbiomac.2019.03.089>
- Kumar, S., & Malviya, R. (2023). Dietary fibers and their derivatives for drug delivery applications: Advances and prospective. *Journal of Drug Delivery Science and Technology*, 89, Article 105084. <https://doi.org/10.1016/j.jddst.2023.105084>
- Li, J., Shang, W. T., Si, X., Bu, D. D., Strappe, P., Zhou, Z. K., & Blanchard, C. (2017). Carboxymethylation of corn bran polysaccharide and its bioactive property. *International Journal of Food Science & Technology*, 52(5), 1176–1184. <https://doi.org/10.1111/ijfs.13382>
- Li, X. L., Thakur, K., Zhang, Y. Y., Tu, X. F., Zhang, Y. S., Zhu, D. Y., ... Z. J. (2018). Effects of different chemical modifications on the antibacterial activities of polysaccharides sequentially extracted from peony seed dreg. *International Journal of Biological Macromolecules*, 116, 664–675. <https://doi.org/10.1016/j.ijbiomac.2018.01.216>
- Li, X. X., Zhang, X. X., Zhang, R., Ni, Z. J., Elam, E., Thakur, K., ... Wei, Z. J. (2021). Gut modulation based anti-diabetic effects of carboxymethylated wheat bran dietary fiber in high-fat diet/streptozotocin-induced diabetic mice and their potential mechanisms. *Food and Chemical Toxicology*, 152. <https://doi.org/10.1016/j.fct.2021.112235>
- Ma, R. H., Zhang, X. X., Ni, Z. J., Thakur, K., Wang, W., Yan, Y. M., ... Z. J. (2023). *Lycium barbarum* (Goji) as functional food: A review of its nutrition, phytochemical structure, biological features, and food industry prospects. *Critical Reviews in Food Science and Nutrition*, 63, 10621–10635. <https://doi.org/10.1080/10408398.2022.2078788>
- Meng, X., Liu, F., Xiao, Y., Cao, J., Wang, M., & Duan, X. (2019). Alterations in physicochemical and functional properties of buckwheat straw insoluble dietary fiber by alkaline hydrogen peroxide treatment. *Food Chemistry: X*, 3, Article 100029. <https://doi.org/10.1016/j.fochx.2019.100029>
- Niu, Y., Li, N., Xia, Q., Hou, Y., & Xu, G. (2018). Comparisons of three modifications on structural, rheological and functional properties of soluble dietary fibers from tomato peels. *LWT*, 88, 56–63. <https://doi.org/10.1016/j.lwt.2017.10.003>
- Pérez-Jiménez, J., Díaz-Rubio, M. E., Mesías, M., Morales, F., & Saura-Calixto, F. (2014). Evidence for the formation of maillardized insoluble dietary fiber in bread: A specific kind of dietary fiber in thermally processed food. *Food Research International*, 55, 391–396. <https://doi.org/10.1016/j.foodres.2013.11.031>
- Qi, J., Li, Y., Masamba, K. G., Shoemaker, C. F., Zhong, F., Majeed, H., & Ma, J. (2016). The effect of chemical treatment on the *in vitro* hypoglycemic properties of rice bran insoluble dietary fiber. *Food Hydrocolloids*, 52, 699–706. <https://doi.org/10.1016/j.foodhyd.2015.08.008>
- Singleton, V. L., Orthofer, R., & Lamuela, R. M. (1999). Analysis of total phenols and other oxidation substrates and antioxidants by means of folin-ciocalteu reagent. In *Methods in enzymology* (pp. 152–178). Elsevier. [https://doi.org/10.1016/S0076-6879\(99\)99017-1](https://doi.org/10.1016/S0076-6879(99)99017-1)
- Song, Y., Su, W., & Mu, Y. C. (2018). Modification of bamboo shoot dietary fiber by extrusion-cellulase technology and its properties. *International Journal of Food Properties*, 21(1), 1219–1232. <https://doi.org/10.1080/10942912.2018.1479715>
- Tan, S., Lan, X., Chen, S., Zhong, X., & Li, W. (2023). Physical character, total polyphenols, anthocyanin profile and antioxidant activity of red cabbage as affected by five processing methods. *Food Research International*, 169, Article 112929. <https://doi.org/10.1016/j.foodres.2023.112929>
- Wang, C. H., Ma, Y. L., Zhu, D. Y., Wang, H., Ren, Y. F., Zhang, J. G., ... Z. J. (2017). Physicochemical and functional properties of dietary fiber from bamboo shoots (*Phyllostachys praecox*). *Emirates Journal of Food and Agriculture*, 509–517. <https://doi.org/10.9755/ejfa.2017-02-274>
- Wang, Y., Xie, Z., Wu, Q., Song, W., Liu, L., Wu, Y., & Gong, Z. (2020). Preparation and characterization of carboxymethyl starch from cadmium-contaminated rice. *Food Chemistry*, 308, Article 125674. <https://doi.org/10.1016/j.foodchem.2019.125674>
- Xu, F., Zhang, S., Zhou, T., Waterhouse, G. I., Du, Y., Sun-Waterhouse, D., & Wu, P. (2022). Green approaches for dietary fibre-rich polysaccharide production from the cooking liquid of Adzuki beans: Enzymatic extraction combined with ultrasonic or high-pressure homogenisation. *Food Hydrocolloids*, 130, Article 107679. <https://doi.org/10.1016/j.foodhyd.2022.107679>
- Xu, Z., Xiong, X., Zeng, Q., He, S., Yuan, Y., Wang, Y., ... Su, D. (2020). Alterations in structural and functional properties of insoluble dietary fibers-bound phenolic complexes derived from lychee pulp by alkaline hydrolysis treatment. *LWT*, 127, Article 109335. <https://doi.org/10.1016/j.lwt.2020.109335>
- Yang, M., Wu, L., Cao, C., Wang, S., & Zhang, D. (2019). Improved function of bamboo shoot fibre by high-speed shear dispersing combined with enzyme treatment. *International Journal of Food Science & Technology*, 54(3), 844–853. <https://doi.org/10.1111/ijfs.14004>
- Yin, W., Liu, M., Xie, J., Jin, Z., Ge, S., Guan, F., ... Liu, J. (2022). Removal of bound polyphenols and its effect on structure, physicochemical and functional properties of insoluble dietary fiber from adzuki bean seed coat. *LWT*, 169, Article 114011. <https://doi.org/10.1016/j.lwt.2022.114011>
- Yu, G., Bei, J., Zhao, J., Li, Q., & Cheng, C. (2018). Modification of carrot (*Daucus carota* Linn. Var. Sativa Hoffm.) pomace insoluble dietary fiber with complex enzyme method, ultrafine comminution, and high hydrostatic pressure. *Food Chemistry*, 257, 333–340. <https://doi.org/10.1016/j.foodchem.2018.03.037>
- Zhang, M. Y., Liao, A. M., Thakur, K., Huang, J. H., Zhang, J. G., & Wei, Z. J. (2019). Modification of wheat bran insoluble dietary fiber with carboxymethylation, complex enzymatic hydrolysis and ultrafine comminution. *Food Chemistry*, 297, Article 124983. <https://doi.org/10.1016/j.foodchem.2019.124983>
- Zhang, S. S., Xu, X. L., Cao, X., & Liu, T. T. (2023). The structural characteristics of dietary fibers from *Tremella fuciformis* and their hypolipidemic effects in mice. *Food Science and Human Wellness*, 12(2), 503–511. <https://doi.org/10.1016/j.fshw.2022.07.052>
- Zhang, Z., Lu, W., Liu, P., Li, M., Ge, X., Yu, B., ... Cui, B. (2023). Microbial modifications with *Lycium barbarum* L. oligosaccharides decrease hepatic fibrosis and mitochondrial abnormalities in mice. *Phytomedicine*, 120, Article 155068. <https://doi.org/10.1016/j.phymed.2023.155068>
- Zhao, X., Chen, J., Chen, F., Wang, X., Zhu, Q., & Ao, Q. (2013). Surface characterization of corn stalk superfine powder studied by FTIR and XRD. *Colloids and Surfaces B: Biointerfaces*, 104, 207–212. <https://doi.org/10.1016/j.colsurfb.2012.12.003>
- Zheng, Y., & Li, Y. (2018). Physicochemical and functional properties of coconut (*Cocos nucifera* L) cake dietary fibres: Effects of cellulase hydrolysis, acid treatment and particle size distribution. *Food Chemistry*, 257, 135–142. <https://doi.org/10.1016/j.foodchem.2018.03.012>
- Zheng, Y., Li, Y., & Tian, H. (2020). Effects of carboxymethylation, acidic treatment, hydroxypropylation and heating combined with enzymatic hydrolysis on structural and physicochemical properties of palm kernel expeller dietary fiber. *LWT*, 133, Article 109909. <https://doi.org/10.1016/j.lwt.2020.109909>
- Zheng, Y., Tian, H., Li, Y., Wang, X., & Shi, P. (2021). Effects of carboxymethylation, hydroxypropylation and dual enzyme hydrolysis combination with heating on physicochemical and functional properties and antioxidant activity of coconut cake dietary fibre. *Food Chemistry*, 336, Article 127688. <https://doi.org/10.1016/j.foodchem.2020.127688>
- Zheng, Y., Wang, X., Sun, Y., Cheng, C., Li, J., Ding, P., & Xu, B. (2022). Effects of ultrafine grinding and cellulase hydrolysis separately combined with hydroxypropylation, carboxymethylation and phosphate crosslinking on the *in vitro* hypoglycaemic and hypolipidaemic properties of millet bran dietary fibre. *LWT*, 172, Article 114210. <https://doi.org/10.1016/j.lwt.2022.114210>
- Zhou, Y., Tang, N., Huang, L., Zhao, Y., Tang, X., & Wang, K. (2018). Effects of salt stress on plant growth, antioxidant capacity, glandular trichome density, and volatile exudates of *Schizonepeta tenuifolia* Briq. *International Journal of Molecular Sciences*, 19(1), 252. <https://doi.org/10.3390/ijms19010252>
- Zhu, Y., Chu, J., Lu, Z., Lv, F., Bie, X., Zhang, C., & Zhao, H. (2018). Physicochemical and functional properties of dietary fiber from foxtail millet (*Setaria italica*) bran. *Journal of Cereal Science*, 79, 456–461. <https://doi.org/10.1016/j.jcs.2017.12.011>